Eur Respir J 2008; 31: 515–522
DOI: 10.1183/09031936.00109407
Copyright©ERS Journals Ltd 2008

Neoalveolarisation contributes to compensatory lung growth following pneumonectomy in mice

H. Fehrenbach*, R. Voswinckel#, V. Michl*, T. Mehling#, A. Fehrenbach*, W. Seeger# and J.R. Nyengaard¶

ABSTRACT: Regeneration of the gas exchange area by induction of neoalveolarisation would greatly improve therapeutic options in destructive pulmonary diseases. Unilateral pneumonectomy is an established model to remove defined portions of gas exchange area and study mechanisms of compensatory lung growth. The question of whether new alveoli are added to the residual lung after pneumonectomy in mice was addressed.

Left-sided pneumonectomy was performed in 11 adult C57BL/6 mice. Alveolar numbers were analysed in lungs fixed at days 6 and 20 after pneumonectomy and in 10 age-matched controls using design-based stereology based on a physical fractionator. Post-fixation lung volume was determined by fluid displacement.

Complete restoration of lung volume was observed 20 days after pneumonectomy. Alveolar numbers were significantly increased by 33% in residual right lungs at day 20 in comparison with control right lungs. In control left lungs, an average of $471 \pm 162 \times 10^3$ alveoli was estimated, 49% of which were regenerated by residual lungs at day 20. Of the newly formed alveoli seen at day 20, 74% were already present at day 6.

The present data demonstrate that, in addition to growth in size of existing alveoli, neoalveolarisation contributes to restoration of the gas exchange area in adult mice and is induced early after pneumonectomy.

KEYWORDS: Alveolarisation, growth, pneumonectomy, pulmonary alveoli, regeneration, septation

Several lung diseases originate from or are associated with a loss of alveolar septa, which may lead to severely compromised gas exchange. Moreover, loss of lung parenchyma results from resection in lung cancer patients or size-reduced lung transplantation in patients with end-stage lung disease [1–3]. Fortunately, the mammalian lung has a high capacity to compensate for major losses of lung tissue. Complete restoration of lung function is achieved either by recruitment of functional reserves or by compensatory lung growth [4]. The formation of new alveoli provides a rationale for identifying intrinsic regenerative programmes of the lung, which may be employed for therapeutic purposes [5, 6].

Resection of major parts of the lung by unilateral pneumonectomy (PNX) is an established model for the study of compensatory lung growth in mammals [4, 7, 8]. As highlighted recently [9], the PNX model has several great advantages: it mimics the loss of functional lung units seen in destructive lung diseases; the loss of tissue is well defined and reproducible; the remaining lung is normal; and compensatory responses can be quantified without difficulty.

Compensatory growth is similar across species, but may differ with age, sex, hormonal status and the amount of lung tissue resected [4, 8]. DNA synthesis and cell proliferation are induced early after PNX in the major resident cell types necessary for generation of new alveolar septa [10–15]. It has recently been demonstrated in adult mice that compensatory lung growth results in the complete restoration of the gas exchanging alveolar septa within 3 weeks [15] and that bone marrow-derived vascular progenitor cells do not contribute to compensatory lung growth in this model [16]. Although detailed quantitative morphological studies demonstrated

For editorial comments see page 483.

AFFILIATIONS
*Clinical Research Group ''Chronic Airway Diseases'', Faculty of Medicine, Philipps University Marburg, Marburg, and,
#Dept of Internal Medicine, University of Giessen Lung Center, Giessen, Germany.
¶Stereology and Electron Microscopy Research Laboratory and MIND Center, University of Århus, Århus, Denmark.

CORRESPONDENCE
H. Fehrenbach
Clinic of Internal Medicine
Clinical Research Group
Philips University
Marburg
Germany
Fax: 49 64212864936
E-mail: heinz.fehrenbach@staff.uni-marburg.de

Received:
August 21 2007
Accepted after revision:
November 05 2007

SUPPORT STATEMENT
H. Fehrenbach is supported by a grant of the Deutsche Forschungsgemeinschaft (FE287/8-1), J.R. Nyengaard is supported by the Danish Council for Strategic Research and the MIND Center is supported by the Lundbeck Foundation, Hellerup, Denmark.

STATEMENT OF INTEREST
A statement of interest for W. Seeger can be found at www.erj.ersjournals.com/misc/statements.shtml

European Respiratory Journal
Print ISSN 0903-1936
Online ISSN 1399-3003

that alveolar and capillary surface area, alveolar septal tissue volume and morphometric lung diffusing capacity are completely restored after PNX [15, 17, 18], the structural basis of how new alveolar tissue is added remains incompletely understood [5]. In particular, it is unclear whether regeneration is accomplished solely by growth of existing alveoli, as indicated by early studies [18–20], or if neoalveolarisation contributes to the restoration of lung parenchyma.

The question whether new alveoli are added or not can be adequately addressed only by means of quantitative morphology. Until recently, the methodological armamentarium did not allow for an unbiased estimation of alveolar numbers. Novel approaches, based on the disector and the fractionator [21, 22], have been established recently for counting alveoli under the microscope without the need for any bias-prone assumptions about their geometry and distribution [23, 24].

In the present study, the contribution of formation of new alveoli to the complete restoration of the alveolar gas exchange area seen after left-sided PNX in mice was assessed [15]. In order to test this hypothesis, a design-based stereologic approach based on the disector and the fractionator was employed to estimate total numbers of alveoli in lungs of mice 6 and 20 days after left-sided PNX and compared with age-matched control mice.

MATERIAL AND METHODS

Animal surgery

As described previously [15], C57BL/6 mice aged 12–14 weeks were anaesthetised and mechanically ventilated with a mouse ventilator (Hugo Sachs Elektronik, March-Hugstetten, Germany). The left lung was lifted through an incision in the 5th intercostal space, tightly ligated at the hilum and resected. Animals were sacrificed at day 6 (n=6) and day 20 (n=5), age-matched controls at day 0 (n=6) and day 20 (n=4). All animal procedures were performed according to the guidelines of good animal experimental practice of the University of Giessen (Giessen, Germany) and approved by the local authorities for animal experiments.

Lung fixation

The architecture of the alveolar gas exchange region in fixed lungs greatly depends upon the mode of fixation used. As perfusion fixation *via* the pulmonary artery at a defined airway pressure was suggested to preserve the alveolar microarchitecture in a state that resembles the situation of the air-filled lung during breathing [25], lungs were fixed by vascular perfusion as described previously [15, 26]. Anaesthetised and heparinised (100 IU) mice were intubated with a 20-G venous catheter (Vasocan® Braunüle® 20 G; B. Braun Melsungen AG, Melsungen, Germany) and mechanically ventilated with a mouse ventilator (MiniVent, Type 845; Hugo Sachs Elektronik). Operations were performed using a Leica MS 5 microscope (Leica Instruments GmbH, Nussloch/Heidelberg, Germany). After sacrifice of the mice with an overdose of halothane, the thoracic cavity was opened, the pulmonary artery was cannulated and the lungs were ventilated through several full ventilation cycles prior to adjustment of a constant airway pressure of 12-cm H_2O column. Then, the lungs were perfused *via* the pulmonary artery with 4% phosphate-buffered paraformaldehyde at a hydrostatic pressure of 15-cm fluid column for 10 min. Trachea and vessels were tightly ligated and excised lungs were stored in cold fixative overnight in a refrigerator.

Sampling of lung tissue using the fractionator

Immediately before sampling, the absolute volume of each lung was determined by fluid displacement [27]. Sampling of tissue blocks and sections was performed according to the method described by HYDE *et al.* [24] which used an orientator to randomise tissue orientation during cutting of 3-mm thick lung slices and subsequent cutting of 3-mm wide bars (fig. 1). Thus, no assumptions were made about the orientation of alveoli within the lung, although the physical fractionator for the estimation of particle numbers is clearly not affected by orientation [21]. Due to the small size of the lungs, all bars obtained were embedded into paraffin so that the bar sampling fraction (SF1) was 1/1.

Embedded bars were cut into 20-μm thick serial sections using a motorised microtome with a block cooling device (H 355 S; Microm, Walldorf, Germany) calibrated for block advance. Sections were collected on slides and haemotoxylin and eosin stained for subsequent estimation of a mean bar thickness of 2,700 μm. The block was then cut down to half of its thickness and a series of eight 5-μm thick serial sections were cut and collected on slides. One central pair of sections was orcein stained for subsequent counting of alveoli. The section sampling fraction (SSF2) is defined by the ratio of serial section thickness/mean bar thickness, *i.e.* 5 μm/2,700 μm=1/540.

Counting of alveoli using the physical disector

All stereological analyses were performed by means of a computer-based system (CAST-Grid 2.1.5; Olympus, Ballerup, Denmark) connected to an Olympus BX-51 microscope. The number of alveoli was determined by estimating the Euler number (χ) of the network of alveolar openings [23, 24]. One pair of orcein-stained sections per tissue block was systematically scanned along the x- and y-axis in order to obtain a uniform, systematic, random sample of disector pairs 600 μm × 600 μm (PNX) to 700 μm × 700 μm (controls) apart. With a counting frame of 24,635 μm^2, the area sampling fraction (ASF3) was 0.0503 (24,635 μm^2/490,000 μm^2) in controls and 0.0684 (24,635 μm^2/360,000 μm^2) in PNX mice, respectively. In order to estimate χ, all bridges, *i.e.* alveolar openings that opened in look-up section but were closed in the reference section of the disector pair, and all islands (I), *i.e.* isolated alveolar edges without connection to alveolar septa in the look-up section and not seen in the reference section, were counted in each counting frame (fig. 2). In each field of view, counting was performed in both directions (double disector) to increase the efficiency of counting. In order to correct for counting frames that could not be evaluated (*e.g.* due to mechanical artefacts to the sections), a correction factor (CF) was introduced. The CF was defined as the ratio of points (upper right corner of the counting frame) hitting distorted lung parenchyma divided by the total number of points hitting lung tissue. As $-\chi$ is the estimator of the number of alveoli in the fraction of lung analysed ($N_{alv,fraction}$), it is calculated according to Equation 1 from the sum of B and the sum of I counted in all disector pairs of an individual lung.

$$N_{alv,fraction} := -\chi = -(\Sigma I - \Sigma B) \times 0.5 \times (1-CF)^{-1} \quad (1)$$

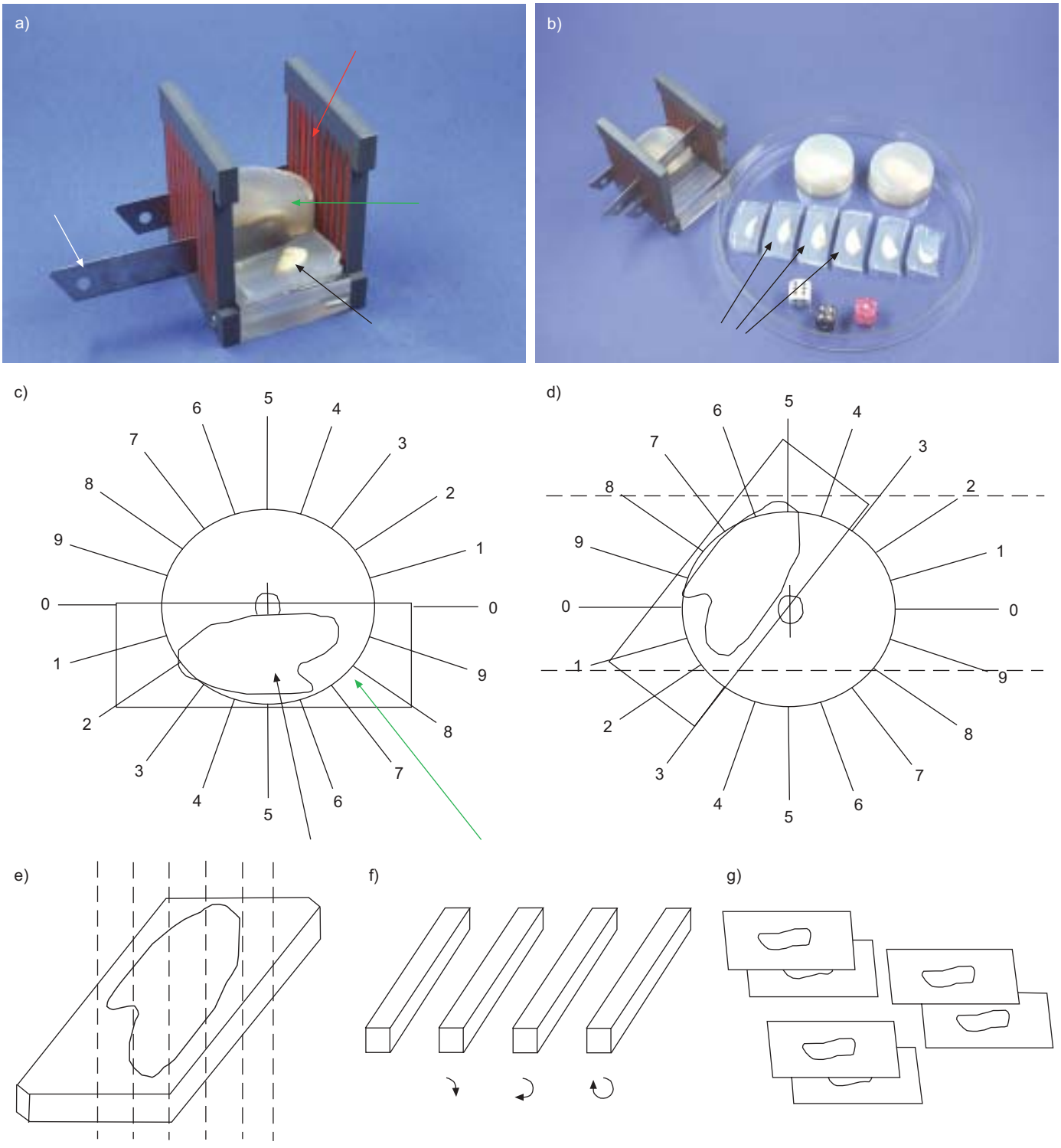

FIGURE 1. Schematic of sampling procedure. a) A left mouse lung embedded into agar (green arrow) is sectioned with a blade (white arrow) into equally sized slices (black arrow) using a matrix (red arrow) with 3 mm spacings. b) Six lung slices (black arrows) surrounded by agar were obtained. c) Each slice was then placed onto an orientator clock to randomise tissue orientation (black arrow: lung slice; green arrow: agar). d) The slice is rotated clockwise so that the original upper edge of the slice is parallel to the line identified by a random number (3 in this example; obtained from a random number table). Cuts, parallel to the horizontal axis (dashed lines) are made in the surrounding agar. e) The slab is then sectioned, using the matrix, into 3-mm thick bars perpendicular (dashed lines) to the new horizontal axis. f) A second random number is used to define the rotational angle (90°, 180°, 270° or 360°) for the first bar and subsequent bars are systematically rotated around the longitudinal axis by increments of +90°. g) The bars were then serially sectioned into 20-µm thick sections (left) and one central pair of 5-µm thick orcein-stained sections (right) used as a disector pair for counting alveoli.

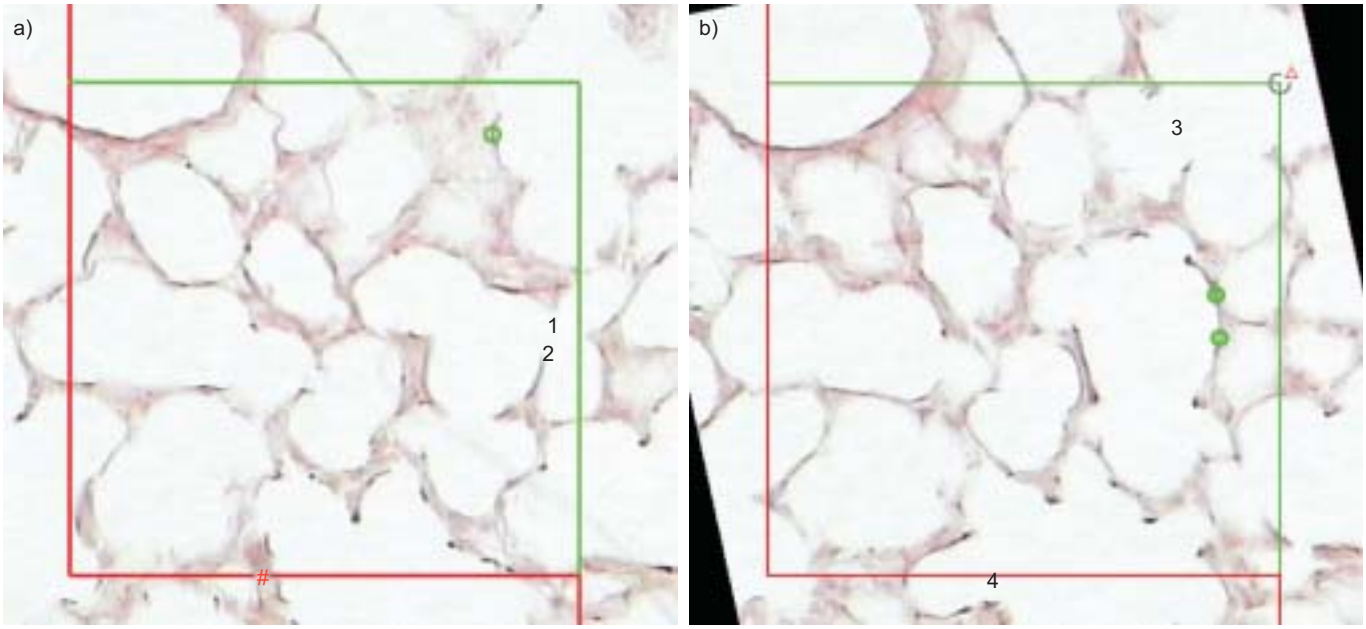

FIGURE 2. Example images showing the process by which bridges and islands are counted. Two corresponding fields of view of a disector pair of orcein-stained sections (a and b) are automatically aligned by the system. In each field of view the sections are overlaid with an unbiased counting frame with an area of 24,635 μm^2. Only those events (green circles: bridges) within the frame or intersecting the inclusion lines (top and right green lines) but not intersecting the exclusion lines (left and bottom red lines) are counted. Bridges are counted if an alveolar opening is closed in one section (green circles) but open in the other (1, 2 and 3). #: this bridge (number 4) intersects an exclusion line and was therefore not counted.

A factor of 0.5 was introduced in Equation 1 because counting was performed in both directions. From this, the total number of alveoli per lung ($N_{alv,lung}$) was calculated according to Equation 2 by multiplication with the inverse of the sampling fractions defined at each sampling step:

$$N_{alv,lung} := -\chi \times (ASF3)^{-1} \times (SSF2)^{-1} \times (SF1)^{-1} \quad (2)$$

Calculating counting noise and variance

In order to evaluate the contribution of the actual counting procedure to the observed variance (OCV), the counting noise (CE_{noise}) was calculated for each lung using Equation 3 according to HYDE *et al.* [24]:

$$CE_{noise}^2 = (\Sigma B + \Sigma I)^{-1} \quad (3)$$

Pilot studies were performed in order to adjust the area sampling fraction by varying the distance between disector pairs so that the mean CE_{noise} was <7%.

OCV was obtained for each experimental group according to Equation 4:

$$OCV(x) = SD(x)/\bar{x} \quad (4)$$

where x represents each experimental group and $\bar{x}$ is the mean.

A mean (range) of 212 (181–284) B was counted in the lungs of 10 control mice and 224 (170–327) B in the lungs of the 11 mice which underwent left-sided PNX. Only one I was observed in all samples. This resulted in an equivalent mean (range) counting noise of 6.9 (5.9–7.4)% in control and 6.8 (5.5–7.7)% in PNX mice.

Statistics

Mean ± SD values are given. One-way ANOVA was performed if normality and equal variance were not rejected ($p>0.1$). A p-value $\leqslant 0.05$ was considered to be statistically significant.

RESULTS

Control mice did not exhibit any significant changes in lung volume during the 20-day period of observation. Total lung volume, determined after vascular fixation with an inflation pressure kept at 12 cmH_2O column, did not differ in control lungs at day 20 *versus* baseline values (table 1). In controls, total post-fixation lung volume amounted to 428 ± 26 mm^3 at day 0 and 437 ± 38 mm^3 at day 20. The volume of the left lung was 157 ± 27 mm^3 at day 0, corresponding to ~37% of total lung volume in control mice. Surgical resection of the left lung was followed by a rapid restoration of organ volume. With a post-fixation right lung volume of 438 ± 65 mm^3, experimental mice had achieved complete restoration of total lung volume at day 20 post-PNX. The volume of the residual right lung was increased by 31% at day 6 post-PNX and 56% at day 20 post-PNX compared with control right lungs.

Using a fractionator design to estimate the χ of the network of alveolar openings (fig. 2), a total of $1{,}165 \pm 145 \times 10^3$ alveoli were estimated for both lungs and a mean number of $471 \pm 162 \times 10^3$ alveoli for the left lung in control mice (table 2). Thus, left-sided PNX removed 40% of the alveoli, which corresponds to a volume fraction of 37% of the left lung.

Compensatory lung growth following PNX resulted in a significant increase in the number of alveoli of the remaining right lung at day 20 compared with right lungs of control mice (fig. 3).

TABLE 1 Post-fixation lung volumes

	Animals n	Lung volume mm^3		
		Left	Right	Total
Baseline, day 0	6	157±27	272±16	428±26
Post-PNX				
Day 6	6		357±50$^{\#}$	357±50$^{\#}$
Day 20	5		438±65¶	438±65
Control, day 20	4	158±30	280±37	437±38
All controls	10	157±27	275±25	432±30

Data are presented as mean±SD, unless otherwise stated. Differences between groups were tested by one-way ANOVA if normality and equal variance were given at p>0.1; otherwise, Kruskal–Wallis one-way ANOVA on ranks was performed. PNX: pneumonectomy. $^{\#}$: p<0.05 *versus* all controls; ¶: p<0.05 *versus* baseline and *versus* control at day 20.

TABLE 2 Stereological estimates of alveolar numbers

	Animals n	Left lung ×10^3	Right lung ×10^3	Total lung ×10^3
Baseline, day 0	6	487±98	643±146	1131±55
Post-PNX				
Day 6	6		866±228	866±228$^{\#}$
Day 20	5		925±150$^{\#,\P}$	925±150
Control, day 20	4	447±247	769±164	1216±228
All controls	10	471±162	694±157	1165±145

Data are presented as mean±SD, unless otherwise stated. Differences between groups were tested by one-way ANOVA if normality and equal variance were given at p>0.1; otherwise, Kruskal–Wallis one-way ANOVA on ranks was performed. $^{\#}$: p<0.05 *versus* all controls; ¶: p<0.05 *versus* baseline.

Notably, the gain in alveoli seen in right lungs was 25% at day 6 post-PNX and 33% at day 20 post-PNX compared with control right lungs. In terms of alveolar numbers, 231×10^3 (49%) of the alveoli removed by left-sided PNX were regenerated (table 2). Notably, 172×10^3 (74%) of the total number of newly formed alveoli present at day 20, were already formed by day 6 post-PNX. Despite the 100% restoration of lung volume at day 20 (table 1), the total number of alveoli of the right lung 20 days after left-sided PNX achieved only 79% of the total alveolar number of both lungs in control mice.

DISCUSSION

Compensatory lung growth following lung resection has been studied in detail in various mammalian species, including mice [15, 16, 28, 29]. These studies indicate that compensatory growth is quite similar across species, although it may differ with age, sex, hormonal status and the amount of lung tissue resected [4, 8]. The nature of alveolar septal growth, however, has been controversially discussed. Some studies reported that the addition of new septa and hence the formation of new alveoli in the residual lung, contributed to the reconstitution of a normal gas exchange area [30], whereas others concluded that compensatory growth was solely, or at least predominantly, achieved by growth in size of the existing alveoli [18, 31]. These early studies were all based on quantitative morphological methods for alveolar counting that are fraught with bias because: only single sections were used; assumptions about specific geometric shapes of alveoli were made; the samples studied were nonuniform; and/or the data were not corrected for shrinkage. WEIBEL and GOMEZ [32], who had developed an earlier method of alveolar counting based on assumptions (*e.g.* about the shape of alveoli), concluded that ''this method has become obsolete with the introduction of the disector, a design-based counting method not requiring any assumption about the structure'' [33].

As highlighted recently [23, 24], the estimation of the number of alveoli poses some methodological problems: 1) alveoli are not discrete, separate particles but constitute a network of saccules opening into an alveolar duct, which precludes to unambiguously define an individual alveolus in a single histological section; and 2) alveoli exhibit an extraordinary diversity in their geometric shape, as demonstrated by three-dimensional acinar reconstructions [34, 35]. Novel approaches, based on the disector and the fractionator principles [21, 22], allow for the unbiased estimation of the number of alveoli under the microscope without the need for assumptions with regard to alveolar shape, size and orientation [23, 24]. The only assumption made is that each alveolar opening ''carries'' one alveolus. Consequently, in the present study an approach was used which is based on systematic uniform random sampling using the fractionator sampling design in conjunction with a physical disector (a three-dimensional probe consisting of two sections a known distance apart) to estimate the χ of the alveolar openings, and hence the number of alveoli, in lungs of mice that underwent left-sided PNX. The fractionator was chosen to avoid any bias introduced by tissue shrinkage during fixation and embedding.

Using this design-based stereological approach, it could be demonstrated that the number of alveoli in 12–14-week-old

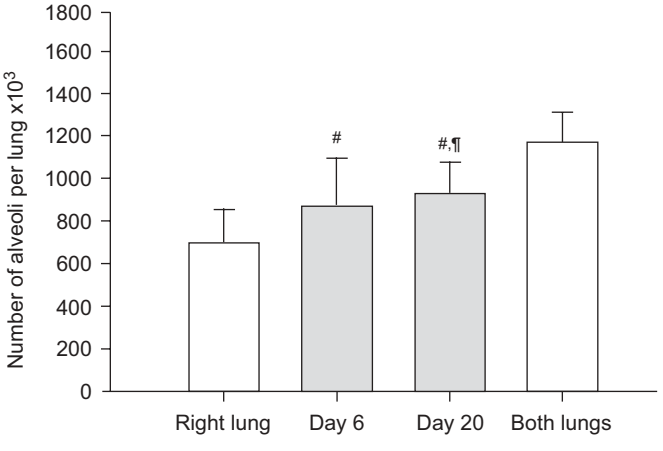

FIGURE 3. Design-based stereological estimation of the numbers of alveoli in right lungs as well as in both lungs of control mice (□) and in residual right lungs of mice at days 6 and 20 after left-sided pneumonectomy (■). Data are presented as mean±SD. $^{\#}$: p<0.05 *versus* control, right lung; ¶: p<0.05 *versus* control, both lungs. Significance tested with one-way ANOVA.

C57BL/6 mice significantly increased in the residual right lung by day 20 post-PNX, which clearly indicates that formation of new alveoli, *i.e.* neoalveolarisation, had occurred. However, the number of new alveoli added to the residual lung compensated for only 49% of the alveoli lost with left lung resection, which is in contrast to the 100% regeneration of organ volume. The present authors have previously demonstrated that restoration of normal lung volume in C57BL/6 mice is accompanied by the complete regeneration of alveolar gas exchange surface area (and total alveolar septal volume), as well as by an increase in the volume–weighted mean alveolar volume [15]. Hence, compensatory lung growth in this murine model is achieved by both addition of new alveoli and growth in size of already existing alveoli.

Notably, 74% of the newly formed alveoli were already present by day 6 post-PNX, which suggests that formation of new alveoli is rapidly induced after lung resection. This is in accordance with several studies [10–15] demonstrating that DNA synthesis and cell proliferation are induced rapidly after PNX in the major resident cell types necessary for generation of new alveolar septa, which is preceded by induction of several transcription factors involved in lung development and repair [28, 29]. As shown previously [15], continuous labelling of proliferating cells over 10 days with bromo-desoxyuridine (BrdU) revealed areas of BrdU-positive, thickened septa in subpleural lung regions, which is in accord with findings of significantly higher proliferation rates in subpleural compared with central lung regions in immature as well as mature dogs undergoing PNX [36]. CAGLE *et al.* [12] demonstrated that proliferation, which was identified by means of autoradiography of injected tritiated thymidine, peaked at day 2 post-PNX in mesothelial cells, whereas alveolar tissue proliferation peaked at day 4. Taken together, these data suggest that formation of new alveoli primarily takes place in subpleural regions of the lung.

The present finding that only 49% of the alveoli removed by PNX were regenerated by day 20, whereas absolute volume of alveolar septal tissue and total alveolar surface area were completely restored [15], indicates that growth in size of already existing alveoli contributes equivalently to compensatory lung growth. This is in accord with *in situ* hybridisation data, which demonstrated tropoelastin and procollagen-I mRNA expression to be uniformly distributed throughout the gas exchange area of rat lungs 3, 7 and 14 days after PNX [37]. Studies in young and adult dogs undergoing right lung PNX revealed that growth of alveolar septa is characterised by an initial disproportionate increase in interstitial cells and matrix by nearly 3.6-fold, whereas epithelial and endothelial cells increase ~2-fold compared with control lungs [14, 38]. Later on, proportions of septal cells gradually normalised resulting in a final 2-fold increase in all compartments relative to age-matched control lungs, and a normal harmonic mean septal barrier thickness and improved lung diffusing capacity were achieved [9].

Alveoli are arranged as lateral chambers along the most peripheral generations of the branched airway tree, which in mice are the alveolar ducts, thus forming an acinus. As was pointed out by SAPOVAL *et al.* [39], efficient gas exchange depends crucially on ensuring adequate oxygen supply to all capillary gas exchange units within the acinus, whether they are centrally located near the entrance or deep at the periphery of the acinus. As oxygen diffuses along the acinar airways, it is progressively extracted at the gas exchange surface along the longitudinal diffusion path, resulting in a progressive decrease of the oxygen partial pressure in a process referred to as screening [39]. Addition of new alveoli at the lung periphery increases the fraction of gas exchange area exposed to low oxygen partial pressure. As central airways appear to adapt slowly and incompletely after PNX [40], enlargement of centrally located alveoli might be a mechanism to increase the fraction of gas exchange area exposed to high oxygen partial pressure and, thus, avoid the unfavourable effect of screening.

Analysis of ventilatory function, performed at ages ranging 2–40 yrs, over a period of >30 yrs in 98 patients with PNX, suggests that compensatory lung growth may play a significant role in children aged <5 yrs, whereas functional adaptation appears to be of major importance in human adults undergoing PNX [41]. This is corroborated by a study in children aged 1 month–11 yrs who underwent lung lobectomy due to pulmonary cystic disease [42]. Pulmonary function analysis performed over two post-operative years indicated that complete normalisation of pulmonary function can be achieved in children aged <4 yrs at the time of operation.

A large body of evidence has been accumulated to support the notion that mechanical strain is the major signal to induce compensatory lung growth in young, as well as mature, individuals provided that the signal is sufficiently strong, and that growth can be modulated by interfering with downstream pathways [4, 5, 8]. This is suggestive of intrinsic programmes that regulate alveolar maintenance, septal growth and neoalveolarisation. The identification of the cellular and molecular mechanisms underlying such intrinsic programmes are of direct clinical relevance, not just after pneumonectomy but also in other pulmonary diseases, such as pulmonary emphysema, to induce regeneration of alveoli [6]. In the era of *in vivo* gene manipulation, mice are the ideal species for the investigation of such regenerative programmes of the lung. However, discovery of the molecular mechanisms actually relevant for neoalveolarisation will depend on the unbiased identification of the formation of new alveoli. This depends on the implementation of design-based quantitative morphology to estimate alveolar numbers.

ACKNOWLEDGEMENTS

The present authors gratefully acknowledge the expert technical assistance of T. Rausch (Clinical Research Group "Chronic Airways Diseases", Faculty of Medicine, Philipps University, Marburg, Germany), N. Weisel and S. Lay (Dept. of Internal Medicine, University of Giessen Lung Center, Giessen, Germany).

REFERENCES

1 Croxton TL, Weinmann GG, Senior RM, Wise RA, Crapo JD, Buist AS. Clinical research in chronic obstructive pulmonary disease: needs and opportunities. *Am J Respir Crit Care Med* 2003; 167: 1142–1149.

2 Edwards JG, Duthie DJ, Waller DA. Lobar volume reduction surgery: a method of increasing the lung cancer resection rate in patients with emphysema. *Thorax* 2001; 56: 791–795.

3 Pierre AF, Keshavjee S. Lung transplantation: donor and recipient critical care aspects. *Curr Opin Crit Care* 2005; 11: 339–344.
4 Hsia CC. Signals and mechanisms of compensatory lung growth. *J Appl Physiol* 2004; 97: 1992–1998.
5 American Thoracic Society. Mechanisms and limits of induced postnatal lung growth. *Am J Respir Crit Care Med* 2004; 170: 319–343.
6 Massaro D, Massaro GD. Toward therapeutic pulmonary alveolar regeneration in humans. *Proc Am Thorac Soc* 2006; 3: 709–712.
7 Cagle PT, Thurlbeck WM. Postpneumonectomy compensatory lung growth. *Am Rev Respir Dis* 1988; 138: 1314–1326.
8 Brown LM, Rannels SR, Rannels DE. Implications of postpneumonectomy compensatory lung growth in pulmonary physiology and disease. *Respir Res* 2001; 2: 340–347.
9 Hsia CCW. Quantitative morphology of compensatory lung growth. *Eur Respir Rev* 2006; 15: 148–156.
10 Brody JS, Burki R, Kaplan N. Deoxyribonucleic acid synthesis in lung cells during compensatory lung growth after pneumonectomy. *Am Rev Respir Dis* 1978; 117: 307–316.
11 Thet LA, Law DJ. Changes in cell number and lung morphology during early postpneumonectomy lung growth. *J Appl Physiol* 1984; 56: 975–978.
12 Cagle PT, Langston C, Goodman JC, Thurlbeck WM. Autoradiographic assessment of the sequence of cellular proliferation in postpneumonectomy lung growth. *Am J Respir Cell Mol Biol* 1990; 3: 153–158.
13 Kuboi S, Mizuuchi A, Mizuuchi T, Taguchi T, Thurlbeck WM, Kida K. DNA synthesis and related enzymes altered in compensatory lung growth in rats. *Scand J Clin Lab Invest* 1992; 52: 707–715.
14 Hsia CC, Herazo LF, Fryder-Doffey F, Weibel ER. Compensatory lung growth occurs in adult dogs after right pneumonectomy. *J Clin Invest* 1994; 94: 405–412.
15 Voswinckel R, Motejl V, Fehrenbach A, *et al.* Characterisation of post-pneumonectomy lung growth in adult mice. *Eur Respir J* 2004; 24: 524–532.
16 Voswinckel R, Ziegelhoeffer T, Heil M, *et al.* Circulating vascular progenitor cells do not contribute to compensatory lung growth. *Circ Res* 2003; 93: 372–379.
17 Hsia CC. Lessons from a canine model of compensatory lung growth. *Curr Top Dev Biol* 2004; 64: 17–32.
18 Sekhon HS, Thurlbeck WM. A comparative study of postpneumonectomy compensatory lung response in growing male and female rats. *J Appl Physiol* 1992; 73: 446–451.
19 Cagle PT, Langston C, Thurlbeck WM. The effect of age on postpneumonectomy growth in rabbits. *Pediatr Pulmonol* 1988; 5: 92–95.
20 Hsia CC, Fryder-Doffey F, Stalder-Nayarro V, Johnson RL Jr, Reynolds RC, Weibel ER. Structural changes underlying compensatory increase of diffusing capacity after left pneumonectomy in adult dogs. *J Clin Invest* 1993; 92: 758–764.
21 Nyengaard JR, Gundersen HJG. Sampling for stereology in lungs. *Eur Respir Rev* 2006; 15: 107–114.
22 Ochs M. A brief update on lung stereology. *J Microsc* 2006; 222: 188–200.
23 Ochs M, Nyengaard JR, Jung A, *et al.* The number of alveoli in the human lung. *Am J Respir Crit Care Med* 2004; 169: 120–124.
24 Hyde DM, Tyler NK, Putney LF, Singh P, Gundersen HJ. Total number and mean size of alveoli in mammalian lung estimated using fractionator sampling and unbiased estimates of the Euler characteristic of alveolar openings. *Anat Rec A Discov Mol Cell Evol Biol* 2004; 277: 216–226.
25 Bachofen H, Ammann A, Wangensteen D, Weibel ER. Perfusion fixation of lungs for structure-function analysis: credits and limitations. *J Appl Physiol* 1982; 53: 528–533.
26 Fehrenbach H, Ochs M. Studying lung ultrastructure. *In*: Uhlig S, Taylor AE, eds. Methods in Pulmonary Research. Basel, Birkhäuser Verlag, 1998; pp. 429–454.
27 Scherle W. A simple method for volumetry of organs in quantitative stereology. *Mikroskopie* 1970; 26: 57–60.
28 Landesberg LJ, Ramalingam R, Lee K, Rosengart TK, Crystal RG. Upregulation of transcription factors in lung in the early phase of postpneumonectomy lung growth. *Am J Physiol Lung Cell Mol Physiol* 2001; 281: L1138–L1149.
29 Zhang Q, Bellotto DJ, Ravikumar P, *et al.* Postpneumonectomy lung expansion elicits hypoxia-inducible factor-1α signaling. *Am J Physiol Lung Cell Mol Physiol* 2007; 293: L497–L504.
30 Langston C, Sachdeva P, Cowan MJ, Haines J, Crystal RG, Thurlbeck WM. Alveolar multiplication in the contralateral lung after unilateral pneumonectomy in the rabbit. *Am Rev Respir Dis* 1977; 115: 7–13.
31 Ibla JC, Shamberger RC, DiCanzio J, Zurakowski D, Koka BV, Lillehei CW. Lung growth after reduced size transplantation in a sheep model. *Transplantation* 1999; 67: 233–240.
32 Weibel ER, Gomez DM. A principle for counting tissue structures on random sections. *J Appl Physiol* 1962; 17: 343–348.
33 Weibel ER, Hsia CC, Ochs M. How much is there really? Why stereology is essential in lung morphometry. *J Appl Physiol* 2007; 102: 459–467.
34 Mercer RR, Crapo JD. Three-dimensional reconstruction of the rat acinus. *J Appl Physiol* 1987; 63: 785–794.
35 Rodriguez M, Bur S, Favre A, Weibel ER. Pulmonary acinus: geometry and morphometry of the peripheral airway system in rat and rabbit. *Am J Anat* 1987; 180: 143–155.
36 Foster DJ, Yan X, Bellotto DJ, *et al.* Expression of epidermal growth factor and surfactant proteins during postnatal and compensatory lung growth. *Am J Physiol Lung Cell Mol Physiol* 2002; 283: L981–L990.
37 Koh DW, Roby JD, Starcher B, Senior RM, Pierce RA. Postpneumonectomy lung growth: a model of reinitiation of tropoelastin and type I collagen production in a normal pattern in adult rat lung. *Am J Respir Cell Mol Biol* 1996; 15: 611–623.
38 Takeda S, Hsia CC, Wagner E, Ramanathan M, Estrera AS, Weibel ER. Compensatory alveolar growth normalizes gas-exchange function in immature dogs after pneumonectomy. *J Appl Physiol* 1999; 86: 1301–1310.
39 Sapoval B, Filoche M, Weibel ER. Smaller is better--but not too small: a physical scale for the design of the mammalian pulmonary acinus. *Proc Natl Acad Sci USA* 2002; 99: 10411–10416.
40 Dane DM, Johnson RL Jr, Hsia CC. Dysanaptic growth of conducting airways after pneumonectomy assessed by CT scan. *J Appl Physiol* 2002; 93: 1235–1242.

41 Laros CD, Westermann CJ. Dilatation, compensatory growth, or both after pneumonectomy during childhood and adolescence. A thirty-year follow-up study. *J Thorac Cardiovasc Surg* 1987; 93: 570–576.

42 Nakajima C, Kijimoto C, Yokoyama Y, *et al*. Longitudinal follow-up of pulmonary function after lobectomy in childhood - factors affecting lung growth. *Pediatr Surg Int* 1998; 13: 341–345.